

Distribution of Corrosion Fatigue Crack Lengths in Carbon Steel*

(2nd Report, The Distributed Cracks which Interact and Coalesce)

By Sotomi ISHIHARA**, Kazuaki SHIOZAWA*** and Kazyu MIYAO****

It has been known that very small distributed cracks can be observed on the surface of smooth specimen subjected to corrosion fatigue, and the fatigue crack growth rate is accelerated by the interaction and coalescence of them.

In this report, following the previous report of the authors, the interaction and coalescence behaviour of the distributed cracks on the specimen surface were observed in detail. Based on the experimental results, distribution of corrosion fatigue crack lengths after a certain cycles can be estimated theoretically. These estimated distributions of crack lengths coincided with those obtained experimentally.

Key Words : Fatigue, Corrosion Fatigue, Carbon Steel, Distributed Cracks, Distribution of Crack Lengths, Crack Coalescence

1. Introduction

It has been known that many small distributed cracks can be observed on the smooth specimen surface subjected to corrosion fatigue, and the crack growth is accelerated by the interaction and coalescence of these cracks. It has also been known [1] that, during fatigue in laboratory air, large cracks are formed by the coalescence of small distributed cracks initiated on the smooth specimen surface, and these cracks propagate unstably and cause the specimen to break. Therefore, in order to estimate fatigue lives whose fatiguing process to fracture are characterized by the crack initiation stage and its growth stage during which small cracks coalesce, it may be important to investigate the growth stage.

In the previous report [2], the authors described the results of corrosion fatigue tests of smooth specimen of carbon steel under plane bedding in salt water and investigation of the crack initiation and growth behaviours of the distributed cracks on the specimen surface in detail, and also examination of the difference of the distribution of crack lengths with stress cycles. It was made clear that the distribution of crack lengths, F , is represented by a mixed type distribution which is composed of a crack group F_1 in which cracks grow as a single crack and a group F_2 in which cracks accelerate their growth by mutual interaction and coalescence with other cracks. Cracks which belong to crack group F_2 are remarkable in the region of high stress ampli-

tude where many cracks are initiated. It was shown that the distribution of crack lengths for crack group F_1 could be derived theoretically from the statistical calculation which took into account the scatter in crack growth rate and the difference of number of cracks initiated during fatigue.

In this report, following the authors previous report [2], the growth behaviours of the cracks belong to the crack group F_2 , and the quantitative evaluation method for group F_2 of cracks was studied. Cracks which belong to F_2 increase their lengths not only by coalescence with each other but also by their own growth. So, in order to consider the two types of crack growth behaviours separately, it is approximated that crack length, $2l$ after a certain number of stress cycles is divided into ρ units of cracks of which length is $2l_a$. The difference of the distribution of unit crack lengths, $2l_a$, with stress cycles is evaluated by the same method as that mentioned in the previous study [2], and for the distribution of ρ , a new model of crack coalescence has been devised. It will be shown that the distribution of crack lengths for F_2 at a certain number of stress cycles can be evaluated by using both models just mentioned. It is made clear that, by superimposing the distribution of crack lengths for F_2 upon that for F_1 obtained in the previous study [2], the distribution of crack lengths for all of the cracks at a certain number of stress cycles and stress amplitude can be introduced.

2. Material and Experimental Procedures

The material tested was a low-carbon steel, JIS SS41, whose chemical composition and mechanical properties were same as those reported in the previous study [2]. Specimen geometry, its dimension and specimen procedures have been already reported in the previous study [2] and are omitted in this paper. Fatigue tests were carried out using a Schenk-type bending machine whose cyclic

* Received 20th January., 1983.

** Assistant, Faculty of Engineering, Toyama University, Toyama 930, Japan.

*** Associate Professor, Faculty of Engineering, Toyama University, Toyama 930, Japan.

**** Professor, Faculty of Engineering, Toyama University, Toyama 930, Japan.

speed is 60 Hz. The environment in the present tests was salt water (3%NaCl) kept at 298 ± 0.5 K, which was dripped at a rate of 20~30 ml per minute on the specimen surface. Other experimental procedures were reported [2][3], so omitted in this paper.

3. Experimental Results and Discussion

3.1 The distribution of both unit crack lengths and number of crack coalescences

As shown in a schematic illustration of Fig. 1, a crack which belongs to F_2 is composed of ρ unit cracks. If crack lengths

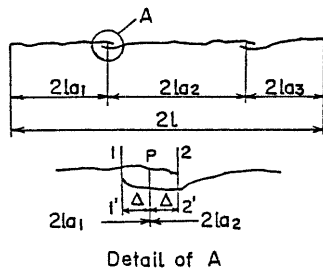


Fig. 1 Definition of unit crack length

for each of these unit cracks are represented by $2l_{ai}$ (designated as unit crack length), crack length, $2l$, is given by the following equation as a total sum of these unit crack lengths.

$$2l = \sum_{i=1}^{\rho} 2l_{ai} \dots \dots \dots (1)$$

In this experiment, as shown in detail of A of Fig. 1, crack lengths, $2l_{ai}$ were measured at the point P which bisected the part ($11' \sim 22'$) where two cracks overlapped as crack tips.

Fig. 2 shows the distribution of unit crack lengths for each stress cycling plotted on the Weibull probability paper. Figs. 2(a) and 2(b) show the results for $\sigma=127$ MPa and 147MPa, respectively. From this figure, it is seen that the distribution of unit crack lengths for both stress amplitudes shifts steadily in the right direction with an increase of stress cycling, and this experimental fact shows that the unit cracks grow for themselves besides being promoted by their coalescence.

Next, variations of density of unit crack, n_a , with stress cycling were investigated. The results for $\sigma=127$ MPa and 147MPa are shown in Fig. 3. As seen from this figure, the increase rate of n_a is large in the early stage of fatigue, but thereafter n_a saturates and settles to a constant values. Therefore, the relation between n_a and N is approximated by the following equation;

$$n_a = n_{a0} \{1 - e^{-\beta_a(N - N_{ca})}\}$$

$$N \geq N_{ca} \dots \dots \dots (2)$$

where, n_{a0} and β_a are the saturated unit crack density and the crack initiation rate for unit crack, respectively. N_{ca} is the number of cycles when the earliest unit crack was initiated, that is, the number of cycles when the first crack coalescence occurred. Experimentally obtained n_a-N equations are shown in this figure. These equations show that the value of β_a for $\sigma=147$ MPa is larger than that for $\sigma=127$ MPa. For this reason, it may be considered that crack coalescence of distributed cracks occurs remarkably in the fatigue process of $\sigma=147$ MPa because crack density initiated during corrosion fatigue process for $\sigma=147$ MPa is five times as large as that for $\sigma=127$ MPa.

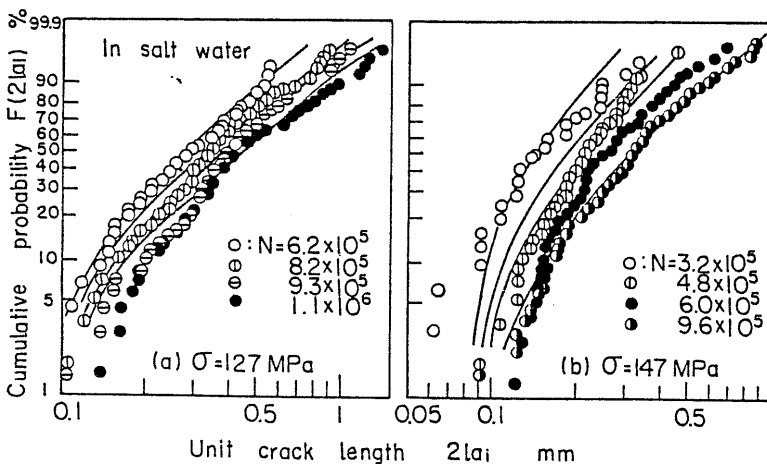


Fig. 2 Change of the distribution of unit crack lengths during corrosion fatigue

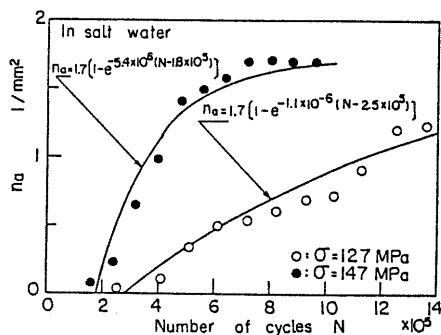


Fig. 3 Change of number of unit cracks per mm^2 during stress cycling in salt water

The distribution of numbers of crack coalescences for all of the cracks which belong to the crack group F_2 was plotted on the Weibull probability paper, and shown in Fig. 4. In this figure, the abscissa represents $\rho-1$. As seen from this figure, the distribution of ρ , $F(\rho)$, does not change remarkably with stress cycling, but slightly shifts in the right direction (the direction in which number of crack coalescences increases). This means that the number of cracks which are composed of many unit cracks increases with stress cycling. This trend was observed independently of stress amplitude. The solid and dotted lines in

this figure will be explained later.

From the experimental results stated above, both the growth by the coalescence with other cracks and that based on the growth of a unit crack must be considered in the quantitative treatment of the crack growth behaviour for the cracks which belong to F₂. A method which considers two types of crack growth behaviours at the same time by pursuing a fixed crack successively is desirable because this method reflects the actuality. But, this may be difficult, and, so, in this study, as stated in the chapter 4, a method in which both the crack growth due to the coalescence and that due to the growth of a unit crack are treated separately will be employed. For this purpose, crack length, $2l$, represented by Eq. (1) is approximated as follows;

$$2l = \sum_{i=1}^n 2l_{ai} \approx \rho \times 2l_a \quad \dots\dots\dots(3)$$

where, $2l_a$ denotes the mean value of unit crack length, $2l_{ai}$.

In order to investigate whether the approximation represented by Eq. (3) is appropriate or not, comparison between the distribution of unit crack lengths shown in Fig. 2 and the distribution of $2l_a$ defined by Eq. (3) is made in Fig. 5 for each stress amplitude and each number of stress cycles. The data points attached with the mark (◊) represent the latter distribution. As seen from this figure, the distribution of unit crack lengths shown in Fig. 2 and the distribution of $2l_a$ defined by Eq. (3) for stress amplitude of $\sigma=127$ and 147 MPa coincide with each other, and the approximation represented by Eq. (3) can be called appropriate.

Next, examinations about whether correlation between $2l_a$ and ρ holds or not were performed for the case, $N=5.6 \times 10^5$ and 8.8×10^5 under stress amplitude of 147 MPa. The results are shown in Fig. 6. From this figure, it is seen that the mean values of $2l_a$ (represented by the mark (O)) at a fixed value of ρ scarcely depend on the number of crack coalescences, ρ . For the case, $N=5.6 \times 10^5$, linear regression between $2l_a$ and ρ was performed and its correlation coefficient turned out to be -0.011 . Therefore, it seems that a remarkable correlation between $2l_a$ and ρ does not exist. Furthermore, χ^2 test was performed by setting a null hypothesis that there was not any statistical correlation between $2l_a$ and ρ , and the following results were obtained: The hypothesis is rejected for 5% level of significance, while it is not rejected for 1% level of significance.

From the above, it may be concluded that, even if a correlation between $2l_a$ and ρ may exist, the degree of the correlation is so low as to be ignored. So, it is possible to suppose that there is no correlation between $2l_a$ and ρ for the first approximation.

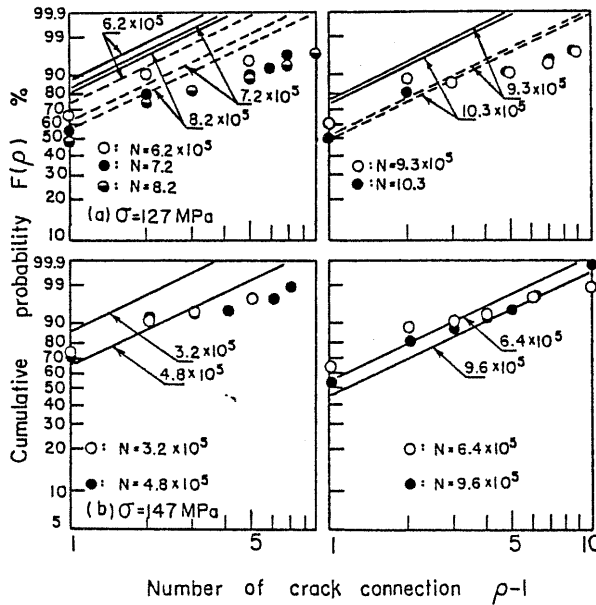


Fig. 4 Variation of the distribution of numbers of crack coalescences during corrosion fatigue

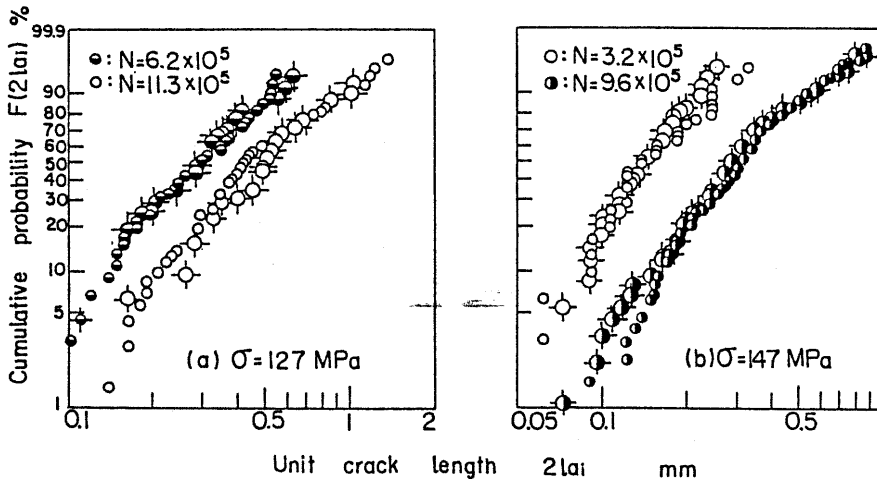


Fig. 5 An approximation of the distribution of unit crack lengths by the distribution of $2l_a$ defined by Eq. (3)

3.2 The growth behaviours of unit cracks

In the previous section, unit crack length $2l_a$ defined by Eq. (3) was introduced by postulating that all of the unit crack lengths, $2l_{ai}$, are equal to one another. In this section, using $2l_a$, the growth behaviours for unit cracks will be investigated. From the previous report [2], crack growth behaviours for the crack group F2 when they grow without their coalescence, that is, crack growth rate under constant value of ρ is given by the following equation.

$$d(2l)/dN = 2C' \dots\dots\dots(4)$$

Substituting Eq. (3) into Eq. (4) and using the condition of $\rho = \text{constant}$, the following equation is obtained.

$$d(2l_a)/dN = 2C'/\rho = C^* \dots\dots\dots(5)$$

Fig. 7 shows variations of unit crack lengths, $2l_a$, during corrosion fatigue for the case of $\sigma = 127 \text{MPa}$. As shown from this figure, $2l_a$ has a nearly linear relationship with stress cycles N under constant value of ρ , and their slopes, C^* , for each crack are different from one another. The correlation between growth rate, C^* , and number of crack coalescences, ρ , was investigated and examples of the results are shown in Fig. 8 for the case of $\sigma = 147 \text{MPa}$. The marks (o) written in this figure indicate the mean value of C^* for a fixed value of ρ , and they show the tendency of decrease with an increasing ρ . But, within the range of this experiment, the degree of its correlation may be so low as to be ignored. Approximating $2l_a$ - N relations as linear relationship, their slopes, C^* , for all of the cracks which belong to F2 were obtained. The distribution of these C^* is plotted on the normal probability paper, and the results are shown in Fig. 9 for the case of $\sigma = 127$ and 147MPa . This figure shows that, though a scatter is somewhat observed in the data, the distribution of C^* is regarded nearly as a normal distribution. The obtained mean value of C^* , \bar{C}^* , and standard deviation of C^* , S_{C^*} , are shown in this figure.

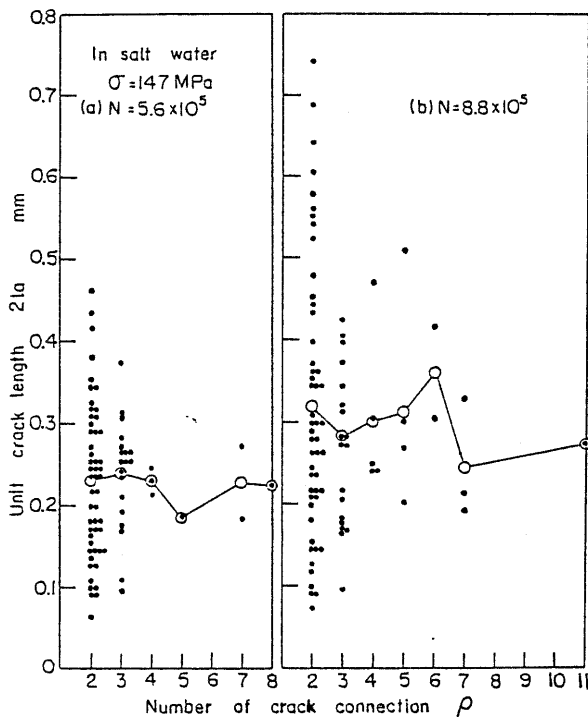


Fig. 6 Examination on correlation between ρ and $2l_a$

4. Derivation of the Distribution of Crack Lengths for the Crack Group F2

In the previous chapter, crack growth behaviours for the cracks which belong to F2 were examined in detail and the following were revealed:

- (i) The cracks which belong to F2 show two kinds of crack growth behaviours: One is the growth by the coalescence with other cracks. The other is the growth for themselves without their coalescence. (ii) The density of unit crack increases with stress cycles N and its change during fatigue process can be described by Eq. (2). (iii) The distribution of unit crack lengths, $2l_{ai}$, can be approximated by that of $2l_a$ defined by Eq. (3). (iv) It can be assumed that

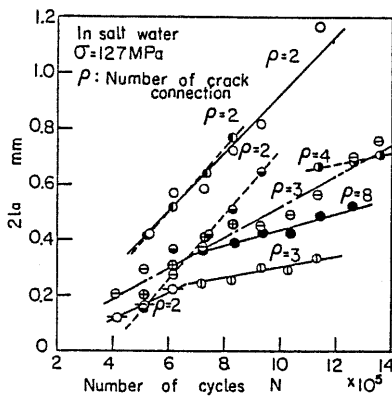


Fig. 7 Variation of the unit crack length ($2l_a$) with stress cycling in salt water

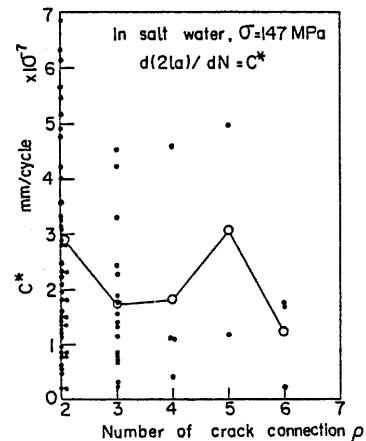


Fig. 8 Examination on correlation between C^* and ρ

number of crack coalescences ρ is independent statistically of unit crack length $2l_a$ defined by Eq. (3). (v) The crack growth law of $2l_a$ is represented by the following equation, $d(2l_a)/dN=C^*$, and the distribution of C^* in this equation is nearly normal.

In this chapter, the calculation method of the distribution of crack lengths for crack group F2 at a certain number of cycles will be studied on the basis of the facts obtained from the experimental observations. We assign $f_1(\rho)$ and $f_2(2l_a)$ as the probabilistic density functions for ρ and $2l_a$, respectively. As investigated in section 3.1, the calculation shown below will be performed considering that there is no correlation statistically between ρ and $2l_a$. In the first place, the probabilistic density function for $2l$ when ρ is constant, $\phi(2l|\rho)$, is represented by using Eq. (3) as follows;

$$\phi(2l|\rho) = f_2(2l_a) \left| \frac{d(2l_a)}{d(2l)} \right| = \frac{1}{\rho} f_2(2l_a) \dots (6)$$

Therefore, the probabilistic density function, $p(2l)$, for all of the values of ρ is given by the following equation,

$$p(2l) = \sum_{\rho=2}^{\infty} \phi(2l|\rho) f_1(\rho) \approx \int_2^{\infty} \frac{1}{\rho} f_2(2l_a) f_1(\rho) d\rho \dots (7)$$

And, distribution function, $F_2(2l)$, will be obtained by integrating Eq. (7) about $2l$ as follows:

$$F_2(2l) = \int_0^{2l} \int_2^{\infty} \frac{1}{\rho} f_1(\rho) f_2\left(\frac{2l}{\rho}\right) d\rho d(2l) \dots (8)$$

If the variations of $f_1(\rho)$ and $f_2(2l_a)$ with stress cycling can be known, the distribution of crack lengths for crack group F2, $F_2(2l)$, at a certain number of stress cycles can be calculated by substituting $f_1(\rho)$ and $f_2(2l_a)$ into Eq. (8). In the following sec-

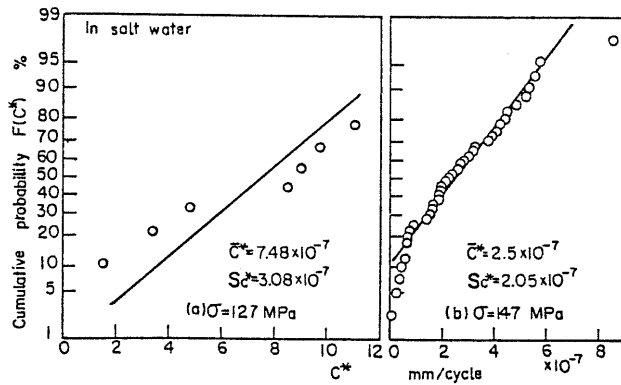


Fig. 9 Distribution of C^* plotted on the normal probability paper

tions, the change of both the probabilistic density function for number of crack coalescences, $f_1(\rho)$, and that for unit crack lengths, $f_2(2l_a)$, with stress cycling will be examined.

4.1 The distribution of unit crack lengths

4.1.1 Calculation method of the distribution of unit crack lengths

The method in this section is basically the same as the one stated in the previous study[2]. The change of unit crack length, $2l_a$, with stress cycling is represented by Eq. (5) as stated in section 3.2. Therefore, by integrating Eq. (5) about N from N_0 to N with the initial condition that $2l_a = 2l_{a0}$ at $N = N_0$, the following equation is obtained;

$$2l_a = C^*(N - N_0) + 2l_{a0} \dots (9)$$

The probabilistic density function of C^* , $f(C^*)$, is considered to have the following normal distribution from experimental results of Fig. 9

$$f(C^*) = \frac{(2\pi S_{C^*}^2)^{-1/2} \exp[-(C^* - \bar{C}^*)^2 / 2S_{C^*}^2]}{\int_0^{\infty} (2\pi S_{C^*}^2)^{-1/2} \exp[-(C^* - \bar{C}^*)^2 / 2S_{C^*}^2] dC^*} \dots (10)$$

where \bar{C}^* and S_{C^*} are the mean value and standard deviation of C^* , respectively. As the probabilistic density function of $2l_a$, $h(2l_a, N)$, is given by the following equation, $h(2l_a, N) = f(C^*) |dC^*/d(2l_a)|$, its final form is given by considering Eqs. (9) and (10) as follows:

$$h(2l_a, N) = \frac{(2\pi S_{2l_a}^2)^{-1/2} \exp[-(2l_a - \bar{C}^*(N - N_0) - 2l_{a0})^2 / 2S_{2l_a}^2]}{\int_{2l_{a0}}^{\infty} (2\pi S_{2l_a}^2)^{-1/2} \exp[-(2l_a - \bar{C}^*(N - N_0) - 2l_{a0})^2 / 2S_{2l_a}^2] d(2l_a)} \dots (11)$$

Hereupon, the following relationships hold between \bar{C}^* , S_{C^*} and $\bar{2l}_a$, S_{2l_a} from Eq. (9).

$$\bar{C}^* = \frac{\bar{2l}_a - 2l_{a0}}{N - N_0}, \quad S_{C^*} = \frac{1}{N - N_0} S_{2l_a} \dots (12)$$

Function $h(2l_a, N)$ given by Eq. (11) represents the probabilistic density function for the length of a crack which is initiated at a number of cycles N_0 and observed at a number of cycles N . Because the relationship between the density of cracks, n_a , and number of cycles N is approximated by Eq. (2) as shown in Fig. 3, the probabilistic density function, $f_2(2l_a, N)$, for all of the cracks that have been initiated until stress cycles N is given as follows:

$$f_2(2l_a, N) = \frac{1}{n_a} \int_{N_{ca}}^N h(2l_a, N) \frac{dn_a}{dN_0} dN_0 \dots (13)$$

And, therefore, the distribution function $F(2l_a, N)$ is obtained by integrating Eq. (13):

$$F(2l_a, N) = \int_{2l_{a0}}^{2l_a} f_2(2l_a, N) d(2l_a) \dots (14)$$

where, $2l_{a0}$ is the smallest half unit crack length measured.

4.1.2 Comparison between numerical results and experimental results

Using both the n_a-N relation shown in Fig. 3 and the mean value, \bar{C}^* , and standard deviation, S_{C^*} , of C^* shown in Fig. 9, Eq. (14) was calculated numerically and the results are shown in Fig. 2 by a solid line. As seen from this figure, the calculated distribution of unit crack lengths coincides well with the experimental results.

4.2 The distribution of numbers of crack coalescences

4.2.1 Calculation method of the distribution of numbers of crack coalescences

Lindborg [4] has already studied the behaviours of crack coalescence for micro cracks. In his paper [4], the behaviours of crack coalescences for micro cracks whose lengths were nearly equal to the dimensions of crystal grains were studied, and so, crack coalescences in not only the direction perpendicular to loading direction but also the direction parallel to loading direction were taken into consideration. But, in this study, the behaviours of crack coalescences for cracks whose lengths are 5~10 times as long as the dimensions of crystal grains will be considered, and so, it is postulated that cracks can coalesce only in the direction perpendicular to loading direction.

The specimen region where cracks will be initiated is divided into m_t cells whose size are equal to one another and whose shape is a regular square of dimension, $2l_a$ as shown in Fig. 10. The following three hypotheses will be used for analysis of the distribution of crack coalescences:

- (i) Distribution of locations of cracks is uniformly random.
- (ii) Cracks increase their lengths only by crack coalescences.
- (iii) Crack coalescence can occur only in the direction which is perpendicular to loading direction.

If the probability that unit crack exists in a certain cell is denoted as λ , the probability that unit crack does not ex-

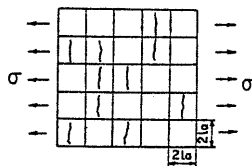


Fig. 10 Coalescence model

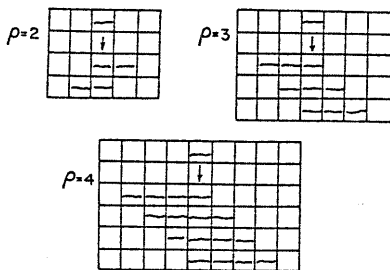


Fig. 11 Various combination methods of unit cracks

ist in a certain cell is written as $1-\lambda$. Therefore, the probability, $q(1)$, that a single crack exists in an observed cell is considered $q(1)=\lambda(1-\lambda)^2$. In the same manner, referring to Fig. 11, the probability, $q(r)$ ($r=1,2,\dots$), that unit crack in an observed cell is a part of the crack whose number of crack coalescences is r is given by the following equations:

$$\left. \begin{aligned} q(1) &= \lambda(1-\lambda)^2 \\ q(2) &= 2\lambda^2(1-\lambda)^2 \\ \dots\dots\dots \\ q(r) &= r\lambda^r(1-\lambda)^2 \\ \dots\dots\dots \end{aligned} \right\} \dots\dots\dots(15)$$

Considering $\sum_{r=1}^{\infty} r\lambda^r = \lambda/(1-\lambda)^2$, summation of $q(r)$, $\sum_{r=1}^{\infty} q(r) = (1-\lambda)^{-2} \sum_{r=1}^{\infty} r\lambda^r$, yields

$$\sum_{r=1}^{\infty} q(r) = \lambda \dots\dots\dots(16)$$

and this coincides with the probability of crack existence, λ . Next, number of coalesced cracks, $\nu(\rho)$, which each consist of ρ unit cracks is given by the following equation.

$$\nu(\rho) = q(\rho) \times (m_t/\rho) \dots\dots\dots(17)$$

And, substituting Eq. (15) into Eq. (17), the following equation is obtained.

$$\nu(\rho) = m_t(1-\lambda)^2 \lambda^\rho \dots\dots\dots(18)$$

In Eq. (18), replacing $\rho=1$, number of cracks which grow as a single crack is obtained.

$$\nu(1) = m_t(1-\lambda)^2 \lambda \dots\dots\dots(19)$$

Number of cracks, $\nu(\rho \geq 2)$, which grow accompanied by crack coalescence is given by the following equation.

$$\nu(\rho \geq 2) = \sum_{r=2}^{\infty} m_t(1-\lambda)^2 \lambda^r = m_t \lambda^2 (1-\lambda) \dots\dots(20)$$

Accordingly, the distribution of numbers of crack coalescences, $F(\rho)$, is given by the following equation.

$$\begin{aligned} F(\rho) &= \sum_{r=2}^{\infty} \{m_t(1-\lambda)^2 \lambda^r / \nu(\rho \geq 2)\} \\ &= 1 - \lambda^{\rho-1} \quad (\rho \geq 2) \dots\dots\dots(21) \end{aligned}$$

Hereupon, transforming Eq. (21), the following equation is obtained.

$$\ln \ln \frac{1}{1-F(\rho)} = \ln(\rho-1) + \ln \ln \frac{1}{\lambda} \dots\dots\dots(22)$$

As seen from this equation, the distribution function, $F(\rho)$, is a three parameters Weibull distribution whose shape, scale and location parameters are 1, $-1/\ln \lambda$ and 1, respectively. Therefore, the probabilistic density function, $f_1(\rho)$, is given by the following equation.

$$f_1(\rho) = \frac{-\ln \lambda \exp\{\ln \lambda(\rho-1)\}}{\int_2^{\infty} [-\ln \lambda \exp\{\ln \lambda(\rho-1)\}] d\rho} \dots\dots(23)$$

A denominator in the above equation is needed because number of crack coalescences, ρ , is equal to or larger than 2. Calculating and simplifying Eq. (23), the following equation can be obtained finally.

$$f_1(\rho) = -\ln \lambda \lambda^{\rho-2} \quad (\rho \geq 2) \dots\dots\dots(24)$$

Next, in order to obtain the probability of crack existence, λ , Eq. (19) was divided by Eq. (20) and the following equation is obtained;

$$\nu(1)/\nu(\rho \geq 2) = (1-\lambda)/\lambda$$

From this equation, λ is obtained as follows;

$$\lambda = \frac{\nu(\rho \geq 2)}{\nu(1) + \nu(\rho \geq 2)} = \frac{\nu(\rho \geq 2)}{\nu(t)} \equiv p_2 \dots\dots\dots(25)$$

where, $\nu(t)$ is number of total cracks and p_2 is the rate of existence for F_2 when the distribution of crack lengths is regarded as a mixed type distribution which consists of F_1 and F_2 .

4.2.2 Comparison between calculated results and experimental results

The distribution of numbers of crack coalescences at a certain number of stress cycles can be calculated by obtaining the probability for crack existence, λ , from Eq. (25) and substituting this into Eq. (21). The calculated results are shown in Fig. 4 by a solid line. As seen from this figure, for the case of $\sigma=147\text{MPa}$ shown in Fig. 4(b), calculated results coincide well with experimental results. For the case of $\sigma=127\text{MPa}$ shown in Fig. 4(a), the tendency that experimentally obtained distribution of numbers of crack coalescences becomes a three parameters Weibull distribution is examined qualitatively, but the calculated results come on the upper side of experimental results and they don't coincide with each other. As the reasons why calculated and experimental results for the distribution of numbers of crack coalescences do not coincide well with each other in the region of low stress amplitudes ($\sigma=127\text{MPa}$), it can be stated that the distribution of locations of cracks is not uniformly random in the region of low stress amplitudes. So, in the next section, the distribution of locations of cracks will be investigated.

4.2.3 Investigation about whether distribution of locations of cracks is uniformly random or not

The distribution of locations of cracks initiated in the area of 130.6mm^2 is shown in Fig. 12 by the points for the case of $\sigma=127\text{MPa}$, $N=9.29 \times 10^5$. The locations of cracks are represented by the central points of the crack length. In order to perform a statistical test, the area was divided into small parts of 1.61mm^2 (whose size is different

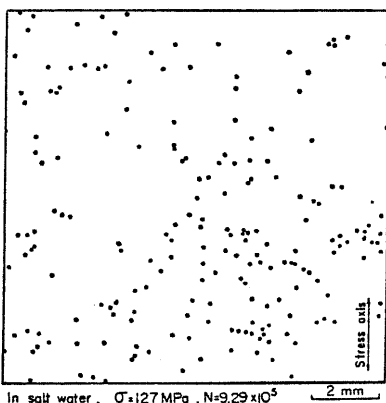


Fig.12 Distribution of locations of cracks in corrosion fatigue for the case of $\sigma=127\text{MPa}$, $N=9.29 \times 10^5$

from that of cell shown in Fig. 10).

If the distribution of locations of cracks is uniformly random and many unit cracks are initiated, the probability that j unit cracks are contained in the observed part can be approximated by the following Poisson distribution;

$$p(j; \mu) = (\mu^j e^{-\mu}) / j! \dots\dots\dots(26)$$

where, μ is the mean value of j . Therefore, the number of parts, M_j , in which j unit cracks are contained is given by the following equation;

$$M_j = M p(j; \mu) = M (\mu^j e^{-\mu}) / j! \dots\dots\dots(27)$$

where, M is the total number of small parts. χ^2 test was performed by setting a null hypothesis that the values of M_j obtained experimentally fit those expected from Poisson distribution, and the following results were obtained: For the case of 127MPa , the hypothesis was rejected for 5% level of significance, and, for the case of 147MPa , it was not rejected for 5% level of significance. From the results stated above, as one of the reasons why calculated and experimental results for distribution of numbers of crack coalescences do not coincide with each other, it can be stated that the distribution of locations of cracks for $\sigma=127\text{MPa}$ is different from random distribution. In the case of $\sigma=127\text{MPa}$, as seen from Fig. 12, cracks are initiated closely in the local region, and so, it may be expected that the probability of crack existence in the local region, λ_l , is larger than that calculated from Eq. (25). Therefore, when cracks are initiated closely in the local region, another method to evaluate the value of λ_l must be devised beside the method in which Eq. (25) is used. For the calculation method of λ_l , let us use the following equation for a while;

$$\lambda_l \approx \Sigma 2l_c / \Sigma 2l_t \dots\dots\dots(28)$$

where, $\Sigma 2l_c$ and $\Sigma 2l_t$ are summation of crack lengths for cracks which belong to F_2 and summation of crack lengths for all of the cracks, respectively. Function $F(\rho)$ was calculated by substituting Eq. (28) into Eq. (21), and the results are shown in Fig. 4(a) by a dotted line. As seen from this figure, calculated and experimental results coincide well with each other. The reason why Eq. (28) may be used to obtain λ_l is considered as follows: Denoting the mean value of number of coalescences by $\bar{\rho}$, $\bar{\rho}$ is given by the following equation.

$$\bar{\rho} = \frac{\sum_{\rho=2}^{\infty} (\rho \times \nu(\rho))}{\sum_{\rho=2}^{\infty} \nu(\rho)} = \frac{2-\lambda}{1-\lambda} \dots\dots\dots(29)$$

Hereupon, if Eq. (29) is applied to the limited local region in the specimen, λ in Eq. (29) may be replaced by λ_l . When the distribution of locations of cracks in the limited local region is uniformly random, Eq. (28) can be transformed as follows.

$$\begin{aligned} \lambda_l &\approx \frac{\Sigma 2l_c}{\Sigma 2l_t} = \frac{\Sigma 2l_c / 2l_a}{\Sigma 2l_t / 2l_a} = \frac{\bar{\rho} \nu(\rho \geq 2)}{\nu(1) + \bar{\rho} \nu(\rho \geq 2)} \\ &= \lambda_l (2 - \lambda_l) \dots\dots\dots(30) \end{aligned}$$

From Eq. (30), the value of λ_l can be obtained as $\lambda_l \approx 1$. Considering that many small cracks are initiated closely in the local region, this value may be nearly appropriate.

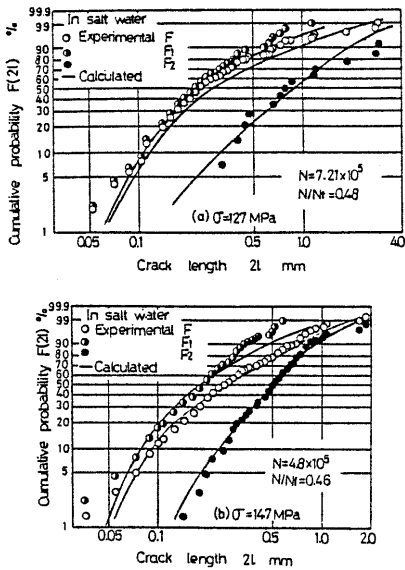


Fig. 13 Comparison between numerical results and experimental results about the distribution of crack lengths

However, when the distribution of locations of cracks is not known and the value of λ_0 is not evaluated, it is necessary to study experimentally whether Eq. (28) should be used to obtain the value of λ_0 or not.

4.3 Comparison between calculated and experimental results for the distribution of crack lengths F

Substituting both the distribution of unit crack lengths and the distribution of number of crack coalescences obtained by using the method stated in section 4.1 and 4.2 into Eq. (8), the distribution of crack lengths, $F_2(2l)$, can be calculated numerically. An example of the results is shown in Fig. 13 for each stress amplitude. The solid line in this figure indicates the calculated results of the distribution of crack lengths for crack group F_1 obtained in the previous report[2]. The distribution of crack lengths for all of the cracks, $F(2l)$, is obtained as the following mixed type distribution, which is composed of $F_1(2l)$ and $F_2(2l)$;

$$F(2l) = p_1 F_1(2l) + p_2 F_2(2l) \dots\dots\dots(31)$$

where, p_1 and p_2 are the rates of existence for F_1 and F_2 , respectively, and their values have been already given in the previous report[2]. The calculated results for $F(2l)$ obtained from Eq. (31) are shown in Fig.13 together with experimental results. As seen from this figure, the calculated and experimental results of the distribution of crack lengths, $F(2l)$, coincide well with each other. Therefore, it is clear that the distribution of crack lengths at a certain stress amplitude and number of stress cycles could be evaluated by the method which took into account both crack initiation and growth behaviours of the distributed cracks.

5. Conclusions

Using smooth specimens of carbon steel,

JIS SS41, plane bending fatigue tests were conducted in salt water (3% NaCl). Crack initiation and growth behaviours for crack group F_2 which grew accompanied with interaction and coalescences with other cracks were investigated in detail and studied to see how they are related to the distribution of crack lengths, F_2 . The results obtained are summarized as follows:

(1) For the crack group F_2 which grows accompanied with interaction and coalescence with other cracks, approximating that crack length $2l$ is composed of ρ unit cracks whose length is $2l_a$, the change of the distribution of $2l_a$ with stress cycles can be explained theoretically by the method which takes both the scatter in growth rate of $2l_a$ and the variation of unit crack density during fatigue into consideration. In this case, crack growth law for unit crack $2l_a$ is represented by $d(2l_a)/dN=C^*$, and C^* in this equation is a probabilistic variable. The distribution of C^* is a normal distribution. And, the change of density of unit crack with stress cycles is given by the following equation, $n_a = n_{a0} [1 - e^{-\rho a(N - N_{ca})}]$.

(2) Postulating that the distribution of locations of cracks is uniformly random and dividing the specimen region into m_t cells whose sizes are equal, the distribution of numbers of crack coalescences, $F(\rho)$, can be explained by a model which defines that crack coalescence occurs when unit cracks exist in the neighbouring cells. From this model, $F(\rho)$ yields a three parameters Weibull distribution whose shape, scale and location parameter are 1, $-1/\ln\lambda$ and 1, respectively, where, λ is the probability that unit cracks exist in the observed cell. For the case of $\sigma=127$ MPa, as the distribution of locations of cracks may not be uniformly random and cracks are initiated closely in the local region, the value of λ for $\sigma=127$ MPa must be determined by considering this experimental fact.

(3) The distribution of crack lengths for all of the cracks, $F(2l)$, at a certain number of stress cycles is obtained as a mixed type distribution, that is composed of both crack group F_1 which grows as a single crack and crack group F_2 which grows accompanied with interaction and coalescence with other cracks. And, the calculated results of $F(2l)$ obtained by taking both crack initiation and growth behaviours of the distributed cracks into consideration coincided well with experimental results.

The authors wish to express their sincere thanks to Professor I. Maekawa of Tohoku University for his helpful advices in the course of this work. And also, they wish to thank Messrs. N. Kawase, A. Yasuda, H. Okajima and S. Fujimoto, who cooperated throughout the experiments.

References

[1] Kitagawa, H., *et al.*, Seisan Kenkyu (in Japanese), 32-1(1980), 31.
 [2] Ishihara, S., *et al.*, Trans. Jpn. Soc. Mech. Engrs. (in Japanese), 50-454, A(1984), 1123.
 [3] Shiozawa, K., *et al.*, J. Soc. Materials Sci. (in Japanese), 27-293(1978), 169.
 [4] Lindborg, U., Acta Met., 17(1969), 521.